An X-ray outflow in a luminous obscured quasar at z≈1.6 in the CDF-S

[Vignali et al. 2015, AA 583, A141]

C. Vignali[1,2], K. Iwasawa[3], A. Comastri[2], R. Gilli[2], G. Lanzuisi[1,2], P. Ranalli[4], N. Cappelluti[5], V. Mainieri[6], I.Georgantopoulos[7], F.J. Carrera[8], J. Fritz[9], M. Brusa[1,2], W.N. Brandt[10], F.E. Bauer[11], F. Fiore[12], F. Tombesi[13]

[(1) University of Bologna; (2) INAF−Osservatorio di Bologna; (3) ICREA and ICC, Universitat de Barcelona; (4) Lund Observatory; (5) Yale University; (6) ESO; (7) National Observatory of Athens; (8) Instituto de Fisica de Cantabria, Santander; (9) UNAM, Mexico; (10) The Pennsylvania State University; (11) Pontificia Universidad Catolica de Chile; (12) INAF-Osservatorio di Roma; (13) NASA Goddard]

Abstract

In the AGN-galaxy co-evolution models, AGN winds and outflows are often invoked to explain why super-massive black holes and galaxies stop growing at a certain phase of their life. Evidences for ultra-fast outflows in X-rays have been collected in the last decade of sensitive XMM-*Newton*, and *Suzaku* observations for a sizable sample of AGN, mostly at low redshift. Here we present deep XMM-*Newton* and *Chandra* data of an obscured (N_H≈a few×10^{23} cm^{-2}) luminous ($L_{2\text{-}10keV}$≈a few×10^{44} erg/s) quasar at z≈1.6 in the *Chandra* Deep Field-South (CDF-S), where an outflow with velocity v_{out}≈0.14c has been significantly detected.

X-ray outflows

Over the last decade, ultra-fast outflows (UFOs, with velocities typically up to 0.1−0.4c) have been clearly detected in X-rays in a sizable sample of AGN, both at low (e.g., Reeves et al. 2003; Pounds & Reeves 2009; Tombesi et al. 2010, 2012; Gofford et al. 2013; Nardini et al. 2015; Tombesi et al. 2015) and high redshift (e.g., Chartas et al. 2002, 2007, 2014; Saez et al. 2009; Lanzuisi et al. 2012). These powerful outflows may provide significant feedback on the quasar host galaxy (e.g., King 2010) and may be responsible for both quenching the star-formation phase and setting up the local Magorrian relation.

Here we present the intriguing properties of source PID352 (as classified in the XMM-*Newton* source catalog in the *Chandra* Deep Field-South (XMM-CDFS; Ranalli et al. 2013). Both XMM-*Newton* and *Chandra* spectral data (taken over a ≈10 yr interval) show the presence of an iron line emission and absorption features. No redshift was available prior to this work. We associated the emission line to neutral iron Kα emission − thus setting **z≈1.6** (lately confirmed by a Keck spectrum) − hence the absorption feature is associated to outflowing highly ionized gas with $\mathbf{v_{out}}$**≈0.14c**. The source is also coincident with a red galaxy placed at the core of a double-lobe Fanaroff-Riley II galaxy. PID352 represents one of the few quasars at high redshift with a detected UFO without being lensed.

XMM-*Newton and Chandra* results

The XMM-*Newton* pn+MOS and *Chandra* ACIS-I spectra of PID352, once fitted with a flat powerlaw, show a clear emission+absorption line complex (**Fig. 1**). Given the absence of a spectroscopic redshift for this source prior to this work (z_{phot}=1.52+0.34/-0.20 at the 95% c.l. from Taylor et al. 2009), we used the emission line to constrain the source redshift. The derived redshift is z=1.59±0.03 (90% c.l.; see **Fig. 2a** for the XMM redshift solution) in case of emission line associated to the neutral FeKα transition. Lately, a redshift z=1.61 was obtained by a Keck near-IR spectrum (**Fig. 2b**) on the basis of the detection of [OIII] and Hα lines. For what concerns the absorption feature (**Fig. 2c**), Monte Carlo simulations indicate that there is 1% probability for this line to be spurious. However, the presence of such feature also in *Chandra* spectrum provides further support to this detection. The EW of the emission and absorption lines are ≈200 eV. The best-fitting XMM-*Newton* spectrum is shown in **Fig. 3**.

To characterize the outflowing wind, we used XSTAR (Bautista & Kallman 2004). The relatively large rest-frame EW of the iron absorption feature, combined with the curve of growth for highly ionized iron transitions (Tombesi et al. 2011), suggests the need for high turbulent velocities; v_{turb}=5000 km/s was then chosen. The resulting column density of the ionized gas and its ionization parameter are in the range N_H=[0.6−5.3]×10^{23} cm^{-2} and Logξ=[2.5−4.4] erg cm/s. The derived outflow velocity due to highly ionized iron (FeXXV Heα at 6.7 keV/FeXXVI Lyα at 6.97 keV) is v_{out}=[0.08−0.16]c. The mass outflow rate is close to the accretion rate of 1.7 $M_\odot$/yr derived considering the AGN bolometric luminosity of ≈10^{46} erg/s from SED fitting. The full list of derived parameters for PID352 is shown in **Table 1**.

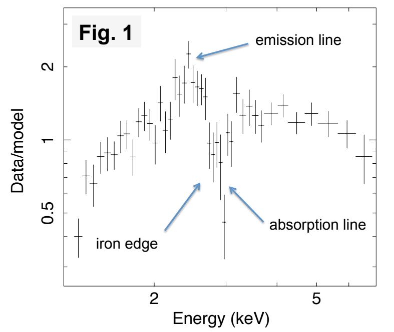

Fig. 1 Observed 1.3−7 keV band spectrum of PID352 divided by the best-fitting powerlaw model (with a flat photon index). The spectral data were made by combining the *XMM-Newton* EPIC pn, MOS1, MOS2, and *Chandra* ACIS-I data. The most relevant spectral features are indicated in the figure.

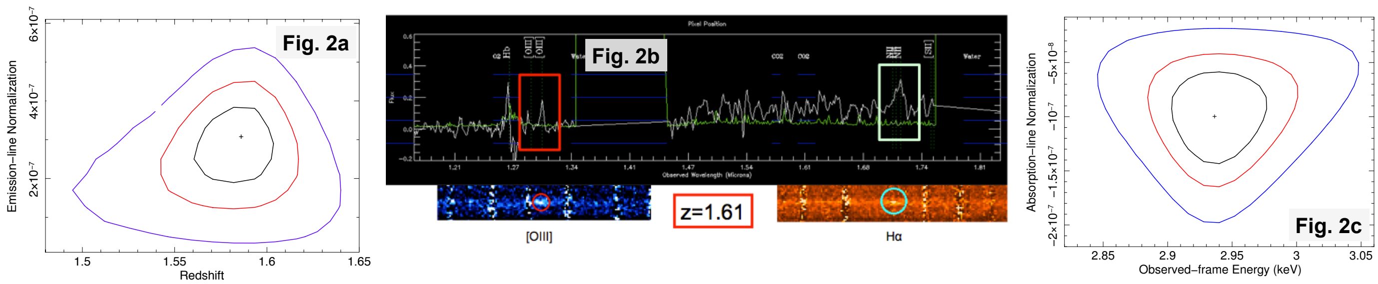

Fig. 2 (a) Redshift solution (obtained using the iron emission line and the absorption edge) vs. line normalization derived using XMM-*Newton* data. The redshift z=1.59±0.03, confirmed by *Chandra* analysis, is consistent with the spectroscopic redshift z=1.61 obtained from Keck (courtesy of G. Hasinger and collaborators; panel **(b)**). **(c)** Absorption line energy vs. normalization. Contours in panels (a) and (c) represent the 68, 90 and 99% confidence level.

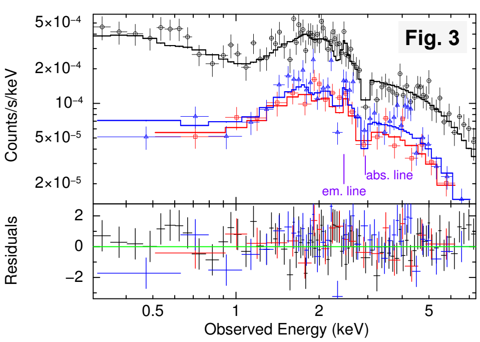

Fig. 3 XMM-*Newton* spectrum of PID352 fitted with a double powerlaw (one absorbed) plus an emission and absorption line. The black/blue/red datapoints refer to pn/MOS1/MOS2 data. Data-to-model residuals are shown in the bottom panel in units of σ.

Table 1 Summarizing table with the main parameters for PID352, including the properties of the outflowing wind. The derived values (see Vignali et al. 2015 for a detailed discussion) suffer from significant uncertainties.

Table 1

$M_{star} \approx 4.9\times10^{11} M_{sun}$ — from SED fitting

$M_{BH} \approx 5.0\times10^{8} M_{sun}$ — (from Sani+11)

$L_{Edd} \approx 6.5\times10^{46}$ erg/s

$L_{bol} \approx 10^{46}$ erg/s — from SED fitting (only accretion component considered here)

$r_{min} = 2GM_{BH}/v_{out}^2 \approx 100R_g$

$\dot{M}_{out} = 4\pi m_p \mu N_H v_{out} r\, Cg$ — Global covering factor~0.5 (from Tombesi) — (from Crenshaw & Kraemer 2012; see also Krongold+07; Pounds & Reeves09)

$\approx 1.7 M_{sun}/yr \approx \dot{M}_{acc}$

Mechanical energy rate

$\dot{E}_{mech} \approx 9.5\times10^{44}$ erg/s $\approx 0.09 L_{bol}$ — Consistent with values required for efficient AGN feedback

$E_{bind} \approx 3.8\times10^{59}$ erg — The energy injected by the wind on the host galaxy may be large on long (Salpeter) timescales

References: •Bautista M.A. & Kallman T.R. 2001, ApJS, 134, 139 •Chartas G. et al. 2002, ApJ, 579, 169 •Chartas G. et al. 2007, Apj, 661, 678 •Chartas G. et al. 2014, ApJ, 783, 57 •Crenshaw D.M. & Kraemer S.B. 2012, ApJ, 753, 75 •Gofford J. et al. 2013, MNRAS, 430, 60 •King A.R. 2010, arXiv:1002.1808 •Krongold Y. et al. 2007, ApJ, 659, 1022 •Lanzuisi G. et al. 2012, A&A, 544, A2 •Nardini E. et al. 2015, Science, 347, 860 •Pounds K.A. & Reeves J.N. 2009, MNRAS, 397, 249 •Ranalli P. et al. 2013, A&A, 555, A42 •Reeves J.N. et al. 2003, ApJ, 593, L65 •Saez C. et al. 2009, ApJ, 697, 194 •Sani E. et al. 2011, MNRAS, 413, 1479 •Taylor E.N. et al. 2009, ApJS, 183, 295 •Tombesi F. et al. 2010, A&A, 521, A57 •Tombesi F. et al. 2011, ApJ, 742, 44 •Tombesi F. et al. 2012, MNRAS, 422, L1 •Tombesi F. et al. 2015, Nature, 519, 436